Open Research Online

The Open University's repository of research publications and other research outputs

Observations of the J = 2 1 line of carbon monoxide in the NGC 2024 nebula

Journal Item

oro.open.ac.uk

Observations of the $J = 2 \to 1$ line of carbon monoxide in the NGC 2024 nebula

G. D. Watt, G. J. White and N. J. Cronin *Molecular Astronomy Group, Physics Department, Queen Mary College, Mile End Road, London E1 4NS*

A. H. F. van Vliet *Astronomy Institute, Utrecht, Holland and Astronomy Division, European Space Agency, ESTEC, Noordwijk, Holland*

Summary. Observations have been made of the $J = 2 \to 1$ transition of ^{12}CO and ^{13}CO in the molecular cloud near NGC 2024. The most intense emission comes from the central regions of the nebula close to areas of high optical extinction. The source contains two hotspots, but no significant velocity gradient or line-broadening was observed. This is consistent with a model in which the emission arises mainly from the high-density interface between the expanding H II region and a neutral cloud. Measurements of the ^{13}CO isotope indicates that $\tau_{13} > 1.7$, but there is insufficient information to derive the density in the region. Analysis of data for Mon R2, however, using the radially collapsing cloud model, indicates a hydrogen density of $\sim 2 \times 10^4 \, cm^{-3}$ for that source.

1 Introduction

NGC 2024 (Orion B) is an H II region lying within the molecular cloud complex L1630. Recent studies of this object (Gordon 1969; Grasdalen 1974; Harper 1974; Macleod, Doherty & Higgs 1975; Hudson & Soifer 1976; Genzel & Downes 1977; Schwartz *et al.* 1977) have shown the presence of a far-infrared source, compact near-infrared sources, high-excitation molecular species, and a water maser source, which indicates that it is, or has recently been, a region of active star formation. In this paper, mapping observations in the $J = 2 \to 1$ transition of CO are presented. $J = 1 \to 0$ CO observations of several positions in NGC 2024 have been reported by Milman (1975) and Kutner *et al.* (1977).

2 Observations

The observations were made during the period 1977 October–November, using the 1.5-m infrared flux collector at Izaña, Tenerife (altitude 2400 m), and an indium antimonide hot-electron-bolometer receiver with system noise temperature ≈ 600 K. The receiver was mounted at the f/13 Cassegrain focus. The observing procedure and details of calibration have been described in White *et al.* (1979).

3 Results

Spectra were taken with a velocity resolution of 1.3 km/s at 37 positions around NGC 2024, centred on the (1950) position RA = $05^h 39^m 14^s$, dec = $-01° 56' 57''$, and with adjacent points typically separated by four arcmin. A map of peak brightness temperature as a function of position is shown in Plate 1. Small linear baselines (typically 0.05 K km/s) were subtracted from 11 of the spectra. From Plate 1, it is seen that there are two hotspot regions surrounded by more diffuse emission along the dust lane which cuts across the optical nebulosity.

The two hotspots are separated by ~ 12 arcmin, corresponding to a projected separation of ~ 1.6 pc at the source distance of 450 pc. Assuming that the kinetic temperature $T =$ 25 K and that the major constituent of the cloud is molecular hydrogen with $n_{H_2} \sim 2 \times 10^5 cm^{-3}$, the Jeans radius for the region is 0.13 pc. Since the separation of the peaks is greater than twice this value, it is probable that each enhancement is a separate condensation.
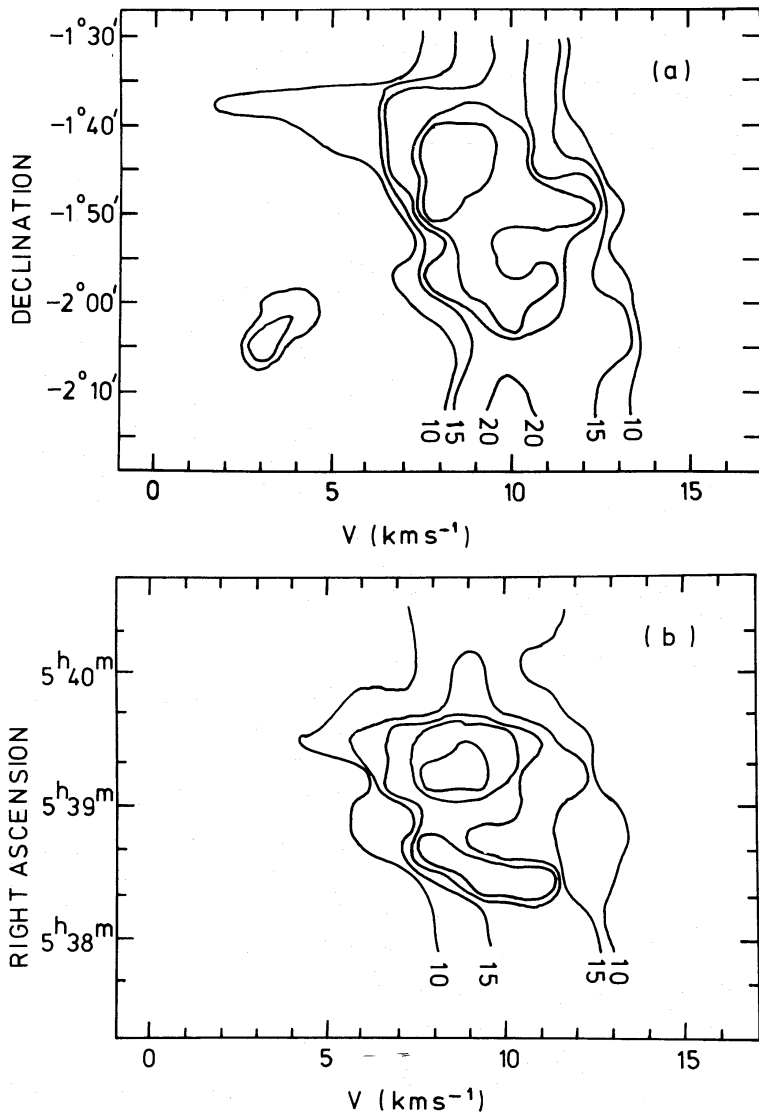

Figure 1. (a) Declination-velocity map of the ^{12}CO line intensity in NGC 2024. The map was made along constant RA = $05^h 39^m 14^s$. The lowest contour level is at 10 K, with intervals of 5 K. The low-velocity features with $V < 6$ km/s are probably due to noise or interference spikes on several bad channels. (b) Right Ascension-velocity map along constant dec = $-01° 44' 57''$. Other details as in Fig. 1(a).
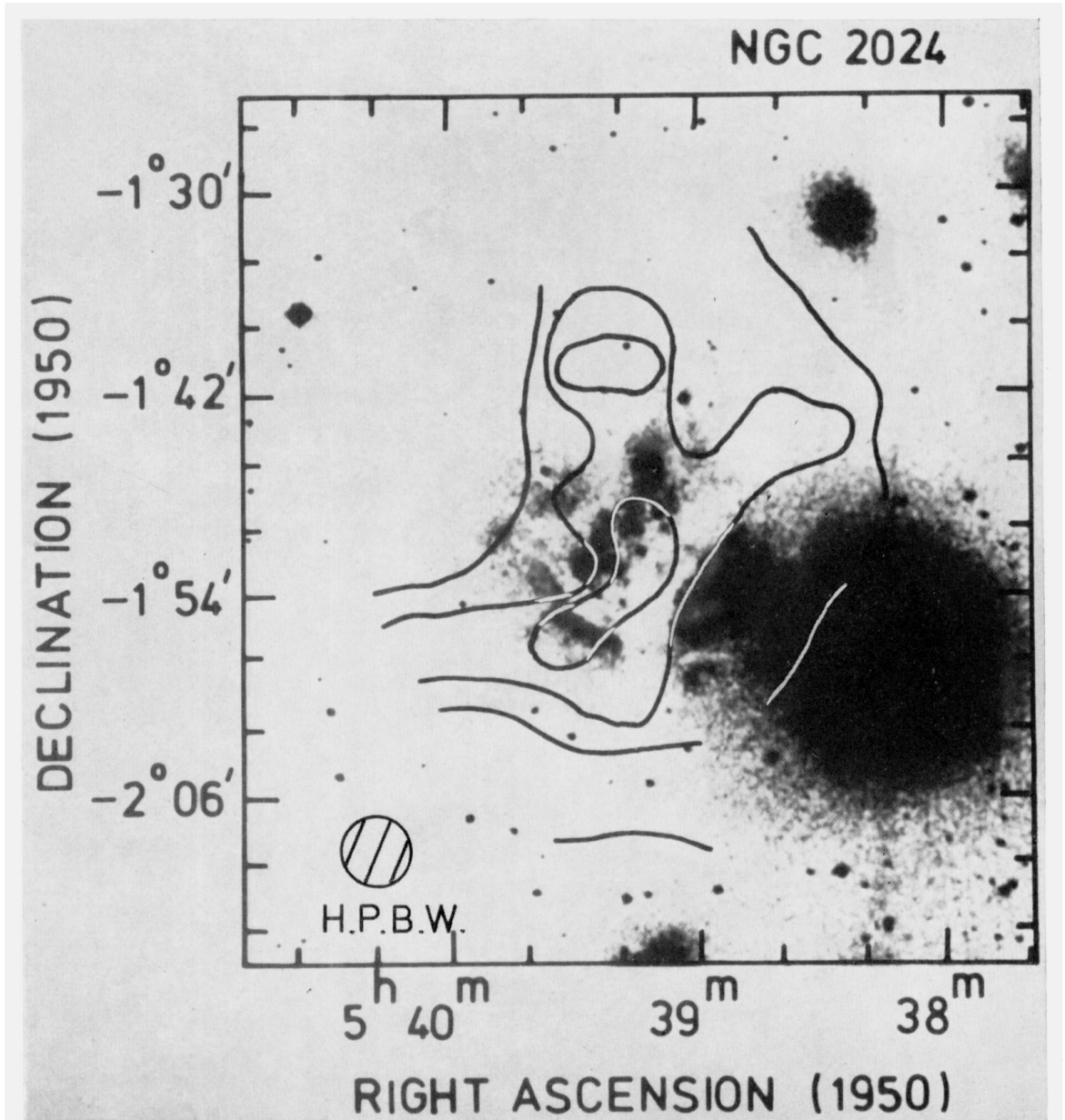
Plate 1. Contours of equal T_b are shown for ^{12}CO, superposed on an optical photograph of the nebula. The lowest contour is at 20 K, the interval is 5 K, and the maximum is 33 K, above the cosmic background of 2.7 K, in the northern hotspot. The half-power beamwidth is 4.5 arcmin.

In Figs 1(a) and (b), maps in the Declination-velocity and Right Ascension-velocity planes are shown. The data are consistent with the H I absorption data of Lockhart & Goss (1978), which show a small velocity gradient across the southern CO hotspot, increasing from north-west to south-east, although further CO data with a higher signal/noise ratio are desirable. The distributions of H I and CO across the source are not similar because the CO molecules tend to lie in regions where hydrogen is present mainly as H_2 molecules. It is clear from these diagrams that little significant line-broadening is observed towards the CO hotspots, or towards nearby infrared or maser sources. This situation may be similar to that described by Lada & Reid (1978), and Elmegreen & Elmegreen (1978) where, instead of molecular hotspots arising from dust cocoons surrounding protostars, we have emission produced in a high-density interface between a diffuse H II region and a dense neutral cloud.

In Fig. 2, spectra of the $J = 2 \rightarrow 1$ ^{12}CO and ^{13}CO isotopes are shown, taken at the point RA = $05^h 38^m 58^s$, dec = $-01° 40' 57''$. Using the method described by White *et al.* (1979), the lower limit to the optical depth of ^{13}CO was estimated to be $\tau_{13} = 1.7 - 0.4 \, (-1\sigma)$.

For a typical cloud density and temperature, the $2 \rightarrow 1$ transition of ^{13}CO is likely to have a larger optical depth than the $1 \rightarrow 0$ transition. The central position of $1 \rightarrow 0$ ^{12}CO and ^{13}CO emission by Goldsmith, Plambeck & Chiao (1975) appears to have been given incorrectly as RA = $05^h 37^m 12^s$. Since this point is well off the source, we assume this position should have been RA = $05^h 39^m 12^s$. In the absence of further $1 \rightarrow 0$ and $2 \rightarrow 1$ ^{13}CO data taken at the same position, we are unable at present to compare optical depths.

For Mon R2 we have recently made numerical calculations, using the radially collapsing cloud model (Goldreich & Kwan 1974) to reproduce the observed ^{12}CO $(2 \rightarrow 1)$ and ^{13}CO $(2 \rightarrow 1)$ intensities given in White *et al.* (1979). Because the isotopic $J = 1 \rightarrow 0$ transitions were observed using a different system with different beamwidth and resolution, we have not attempted to match data but have adjusted the parameters to reproduce the observed ratio of intensities $^{13}CO(1 \rightarrow 0)/^{12}CO(1 \rightarrow 0) = 0.47$. The observations are satisfied for a small range of values centred on $n_{H_2} = 2.0 \times 10^4 \, cm^{-3}$, and $n_{CO} = 0.7 \, cm^{-3}$, assuming a kinetic temperature of $T = 32$ K, an isotope ratio $^{12}C/^{13}C = 40$, and a velocity gradient of $2 \, km \, s^{-1} \, pc^{-1}$. These parameters produce an optically thin $1 \rightarrow 0$ ^{13}CO transition $(\tau = 0.3)$ and an optically thick $J = 2 \rightarrow 1$ ^{13}CO transition $(\tau = 2.0)$.
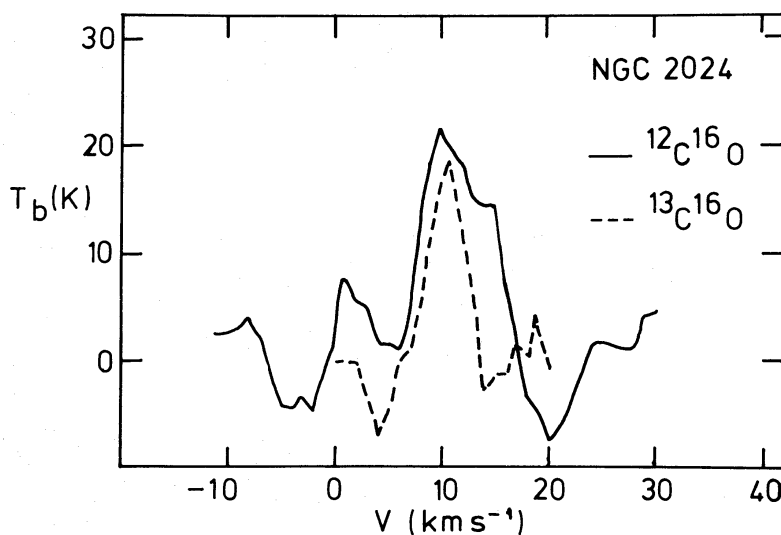

Figure 2. ^{12}CO and ^{13}CO spectra from NGC 2024. The ^{12}CO spectrum has been smoothed to 2.6 km/s resolution. The ^{13}CO spectrum has been smoothed to 1.3 km/s resolution. The temperature scale is the brightness temperature above the cosmic background.

In the systematic radially collapsing model used above, the ^{13}CO intensities are lower than those of the thermalized ^{12}CO transitions because of a lower abundance of the isotope. The hydrogen density in the cloud does not produce a sufficiently high collision rate for the ^{13}CO molecules to thermalize the line at the kinetic temperature. In the case above, the ^{13}CO $2 \rightarrow 1$ excitation temperature was found to be $26\,K$ compared with a kinetic temperature of $32\,K$. However, the data are also consistent with clumping models (Plambeck, Williams & Goldsmith 1977) in which the ^{12}CO is distributed uniformly throughout the cloud in its optically thick state, whilst the ^{13}CO is thin except in 'knots' of high density and/or temperature, which have projected areas of less than the telescope beamwidth. Within these knots, the previous statement that $\tau_{2 \rightarrow 1} > \tau_{1 \rightarrow 0}$ will still hold, and when the knots are averaged over the beam, we should still maintain a high $\tau_{2 \rightarrow 1}$, with the line intensity for the ^{13}CO transitions reduced by a filling factor (f) from that of the ^{12}CO transitions, similar to the NH_3 model by Schwartz *et al.* (1977). The value of f can be determined from the ratio of $^{13}CO/^{12}CO$ intensities, and should be constant for all transitions observed within the source.

Plambeck & Williams (1978) have used $J = 2 \rightarrow 1$ ^{13}CO and $C^{18}O$ intensities to predict hydrogen densities in several molecular cloud regions. However, they use a CO abundance $\sim 10^{-4}$, a factor of ~ 10 higher than the most commonly used values. Since the intensity of CO emission is roughly proportional to the total number of CO molecules, it is reasonable that their value for n_{H_2} in the Mon R2 region is a factor of 10 lower than ours. This lower abundance of CO is obtained from two assumptions. Firstly, that the average cosmic ratio $C/H \sim 3 \times 10^{-4}$ applies in the region, and secondly that only 10 per cent of the C is bound in CO molecules. Both of these values are uncertain at present and probably vary from source to source.

4 Conclusion

Mapping observations in the $J = 2 \rightarrow 1$ transition of ^{12}CO in NGC 2024 reveal the presence of two hotspots separated by ~ 12 arcmin. A comparison of the ^{12}CO and ^{13}CO intensities indicates that the ^{13}CO line is optically thick, although there is insufficient information to determine the hydrogen density. Analysis of previous data for Mon R2, using a radially collapsing cloud model, indicates a hydrogen density $\sim 2 \times 10^4 \, cm^{-3}$. The data from these two sources are consistent with clumping models, and suggest the existence of small-scale structure.

References

Elmegreen, D. M. & Elmegreen, B. G., 1978. *Astrophys. J.,* **219**, 105.
Genzel, R. & Downes, D., 1977. *Astr. Astrophys. Suppl.,* **30**, 145.

Goldreich, P. & Kwan, J., 1974. *Astrophys. J.,* **189**, 441.

Goldsmith, P. F., Plambeck, R. L. & Chiao, R. Y., 1975. *Astrophys. J.,* **196**, L39.

Gordon, M. A., 1969. *Astrophys. J.,* **158**, 479.

Grasdalen, G. L., 1974. *Astrophys. J.,* **193**, 373.

Harper, D. A., 1974. *Astrophys. J.,* **192**, 557.

Hudson, H. S. & Soifer, B. T., 1976. *Astrophys. J.,* **206**, 100.

Kutner, M. L., Tucker, K. D., Chin, G. & Thaddeus, P., 1977. *Astrophys. J.,* **215**, 521.

Lada, C. J. & Reid, M. J., 1978. *Astrophys. J.,* **219**, 95.

Lockhart, I. A. & Goss, W. M., 1978. *Astr. Astrophys.,* **67**, 355.

Macleod, J. M., Doherty, L. H. & Higgs, L. A., 1975. *Astr. Astrophys.,* **42**, 195.

Milman, A. S., 1975. *Astrophys. J.,* **202**, 673.

Plambeck, R. L. & Williams, D. R. W., 1978. *Astrophys. J. Lett.,* preprint.

Plambeck, R. L., Williams, D. R. & Goldsmith, P. F., 1977. *Astrophys. J.,* **213**, L41.

Schwartz, P. R., Cheung, A. C., Bologna, J. M., Chui, M. F., Waak, J. A. & Matsakis, D., 1977. *Astrophys. J.,* **218**, 671.

White, G. J., Watt, G. D., Cronin, N. J. & van Vliet, A. H. F., 1979. *Mon. Not. R. astr. Soc.,* **186**, 107.